RSC Advances

ROYAL SOCIETY OF CHEMISTRY

www.rsc.org/advances

Journal Name

ARTICLE

Band Modification of Graphene by Using Slow Cs^+ Ions

Sijin Sung,[a] Sang-Hoon Lee,[a] Paengro Lee,[a] Jingul Kim,[a] Heemin Park,[a] Mintae Ryu,[a] Namdong Kim,[b] Choongyu Hwang,[c] Seung-Hoon Jhi,[a] and Jinwook Chung[a]†

Received 00th January 20xx,
Accepted 00th January 20xx

DOI: 10.1039/x0xx00000x

www.rsc.org/nanoscale

We report new wide band gap engineering for graphene by using slow Cs^+ ions that allows both fine-tuning and on-off switching capability of the band gap in a range suitable for most applications without modifying or deteriorating the relativistic nature of Dirac fermions. The doping of Cs^+ ions opens a band gap up to E_g=0.68 eV, which can be closed completely by adding neutral Cs atoms as observed in angle-resolved photoemission spectroscopy measurements. The operating mechanism of this band gap engineering is understood by a simple capacitor model, which is fully supported by our density-functional theory calculations.

1. Introduction

Graphene, a single atomic layer of graphite, still remains as a tantalizing candidate to be utilized in electronic applications mainly due to its linear gapless band spectrum.[1–4] This gapless semi-metallic nature of graphene, however, has to be converted into a semiconducting phase with a finite band gap (E_g) to control the conductivity in most electronic applications.[5–9] Since the massless Dirac fermions in graphene showing ballistic charge transport even at room temperature are ideal charge carriers for fast circuit devices, research efforts have been continued to open a tunable band gap in graphene. To this end, there have been continuing efforts to realize the band gap in graphene by using several different schemes, for example, by using graphene nanoribbons,[10,11] bilayer graphene,[12,13] and the functionalized graphene.[14,15] As described in earlier papers, each method has its own merits, but none so far seems to offer a stable and tunable band gap with an on/off switching capability for device applications. Because of its diversity and feasibility, the functionalized graphene has been extensively adopted to open a band gap at the K-point (k =1.7 $Å^{-1}$) of the Brillouin zone essentially by lifting the symmetry between the two sublattices (A and B) of graphene with external adatoms[15,16] or admolecules.[17,18] One of the crucial drawbacks of this method, however, is the adsorbate-induced degradation of the exotic properties of graphene such as the severe lattice distortions predicted for the hydrogenated graphene,[19] and the reduced mobility of the charge carriers.[20] With slow alkali metal ions, however, graphene may be functionalized with no such drawbacks by avoiding the strong covalent hybridization with the sp^2 orbitals of graphene.[21,22]

Here we report an efficient route to functionalize graphene to create a tunable band gap in graphene by using a low-energy beam of Cs^+ ions. Without causing any detectable adverse effect on the intrinsic properties of graphene, we find a rather easy and reproducible means not only to form a band gap in graphene, but also to accurately control its size up to E_g=0.68 eV by varying the dose of Cs^+ ions. We further demonstrate that one may establish the on/off switching capability of the band gap by mixing Cs^+ ions with neutral Cs atoms in a proper sequential order. We have observed evidence of these features both in the linear π-band of graphene and the C 1s and Cs 4d core levels from a single layer graphene (SLG) formed on SiC(0001) surface by using angle-resolved photoemission spectroscopy (ARPES) and high-resolution core level spectroscopy (HRCLS) with synchrotron photons.

[a] Department of Physics, Pohang University of Science and Technology, Pohang 790-784, Korea
[b] Beamline Research Division, Pohang Accelerator Laboratory, Pohang 790-784, Korea .
[c] Department of Physics, Pusan National University, Busan 609-735, Korea
[d] † Corresponding author, E-mail: jwc@postech.ac.kr
[e] Electronic Supplementary Information (ESI) available: [details of any supplementary information available should be included here]. See DOI: 10.1039/x0xx00000x

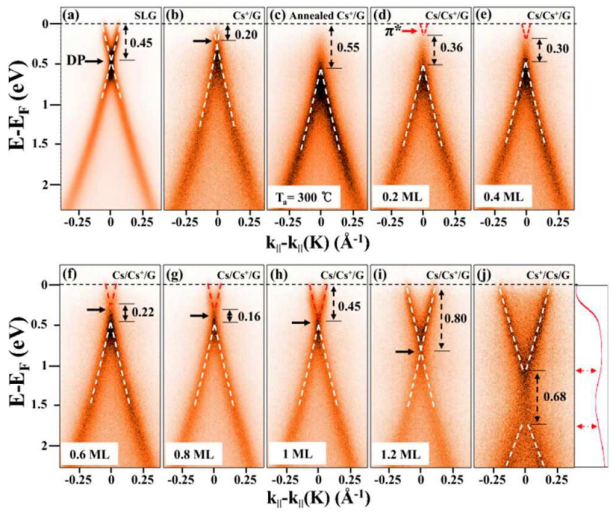

Fig. 1 Opening and fine-tuning a band gap in the π-band of graphene. The changes in the π-band of graphene upon different surface treatments with Cs^+ ions and neutral Cs atoms; (a), SLG, (b), Cs^+ ions doped (1.0 ML) graphene (Cs^+/G), (c), annealed Cs^+/G at 300 °C, (d)–(i), Cs added Cs^+/G (Cs/Cs^+/G) with increasing ϑ_{Cs}, and (j), Cs^+ ion deposited on Cs pre-adsorbed graphene (Cs^+/Cs/G). These bands were measured by using synchrotron photons of energy 34 eV with the samples maintained at 85 K. A band gap E_g=0.55 eV is found in (c) when the Cs^+/G is annealed, and the size of E_g decreases gradually with increasing ϑ_{Cs} until it completely vanishes at ϑ_{Cs}=1.0 ML, demonstrating the on/off switching feature of the band gap. In (j), additional Cs induces an n-doping for the DP, and opens a band gap up to E_g=0.68 eV when Cs^+ ions are doped again. The energy distribution curve (EDC; red curve) shows reduced intensity within the gap.

Our scanning tunneling microscopy (STM) images for the Cs^+-doped SLG show a preferred direction in the charge density, indicative of a symmetry breaking for the two sublattices. By devising a parallel-plate capacitor model to simulate the Cs^+-doped graphene, we have carried out our density functional theory (DFT) calculations, which account for most of our experimental observations associated with the band gap.

2. Results and Discussion

2.1. Cs^+ Ion-Induced Band Gap in the π-Band of Graphene

Figure 1 shows the changes in the linear π-band of SLG upon surface treatments with Cs^+ ions or neutral Cs atoms obtained from (a) SLG, (b) 1.0 monolayer (ML) Cs^+ ions doped graphene (Cs^+/G), (c) annealed Cs^+/G at 300 °C, (d)-(i) Cs added Cs^+/G (Cs/Cs^+/G) with increasing Cs coverage ϑ_{Cs}, and (j) Cs^+ ion deposited on Cs pre-adsorbed graphene (Cs^+/Cs/G). These bands were obtained along the direction perpendicular to the Γ→K direction with the center at the K-point. The best fit bands to locate the top (bottom) of the π-(π*-) band are depicted as white dashed lines in Fig. 1 drawn by determining the slopes of the bands from the neighboring momentum distribution curves (MDCs) obtained at two different energies near the Dirac point (DP).

The π-band from a clean SLG in Fig. 1a shows the DP at 0.45 eV below the Fermi level by the n-doping effect from the substrate.[23] The DP then shifts up by about 0.2 eV when Cs^+ ions of 1 ML with an energy of 100 eV are deposited on the SLG (see Fig. 1b) by a p-doping effect, which is also seen from the Ar^+ ions deposited graphene[24] due to the reduced charge transfer near the Cs^+-induced defects. Interestingly, we can rather easily control the position of DP by adjusting the amount of Cs^+ ions on graphene. The DP drastically changes when this Cs^+/G sample is annealed at T_a=300 °C (Fig. 1c), where the top of the π-band is shifted down by 0.35 eV with no visible conduction (π*-) band, apparently signifying the opening of a band gap $E_g \geq 0.55$ eV. As we add neutral Cs atoms (ϑ_{Cs}=0.2 ML) on the annealed sample to form a Cs/Cs^+/G sample, the minimum of the π*-band (red dashed lines) begins to appear as seen in Fig. 1d showing a reduced E_g=0.36 eV. The size of the band gap gradually decreases with increasing ϑ_{Cs}, and eventually vanishes at ϑ_{Cs}=1.0 ML when the tips of π- and π*-band meet at the DP (Fig. 1h). The DP continues to shift down with ϑ_{Cs}>1.0 ML reaching, for example, to 0.80 eV away from the Fermi level for ϑ_{Cs}=1.2 ML (Fig. 1i).

2.2. Persistent Dirac Nature and Switching Capability of the Band Gap

We further demonstrate that not only the size of the band gap but also the position of the DP can be artificially controlled by adjusting ϑ_{Cs} of neutral Cs atoms prior to the deposition Cs^+ ions on graphene. In Fig. 1j, we have deposited Cs^+ ions (1.0 ML) on the Cs pre-adsorbed graphene (ϑ_{Cs}=1.2 ML), where one finds E_g=0.68 eV when the sample is annealed at T_a=300 °C. The Cs pre-adsorbed SLG shows the DP at 1.4 eV below the Fermi energy with some intensity nearby the DP due probably to in-gap states or to many-body interactions as debated earlier.[25-29] It is important to note that the opening of such a band gap is found to affect little to the intrinsic nature of the π-band as seen by the estimated Fermi velocity v_F =0.94±0.05×10^6 m s^{-1}, which is reduced slightly from 1.07±0.02×10^6 m s^{-1} of the SLG in Fig. 1a while maintaining the linear dispersion. The coverage of pre-adsorbed Cs on graphene thus determines the

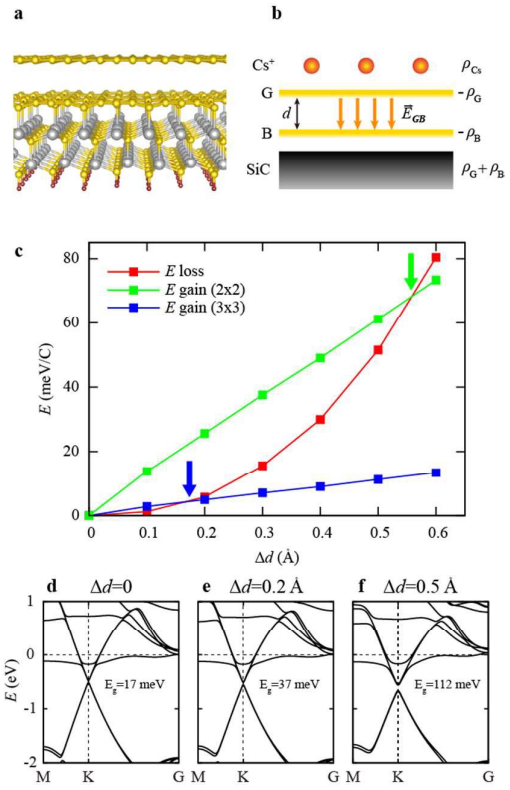

Fig, 2 DFT band calculations based on the capacitor model. (a), The optimized atomic structure of graphene grown on SiC(0001) surface. Gray balls (Si), yellow balls (C), brown balls (H). (b), A parallel plate capacitor model representing the Cs^+-doped graphene (G) on SiC(0001) where *d* is the graphene-buffer layer (B) distance, and E_{GB} is the electric field between them. The charge density of Cs^+ ions, graphene, buffer layer, and SiC surface is represented by ρ_{Cs}, $-\rho_G$, $-\rho_B$, and $\rho_G+\rho_B$, respectively. (c), Changes in the energy loss (red squares) and gain (green and blue) as Δd increases, where one finds the energy-balanced distance change of Δd=0.55 (green arrow) and 0.17 Å (blue arrow) by one Cs^+ ion per 2×2 and 3×3 supercells, respectively. (d)–(f), Changes in the band structures with increasing Δd, showing the gradual increase of a band gap up to 112 meV for Δd=0.5 Å.

position of DP, the mid-gap or Dirac energy of the band gap, while the amount of Cs^+ ions deposited determines the size of the band gap itself. We thus demonstrate the opening and closing of the band gap in graphene, thermodynamically stable up to temperature as high as 300 °C, by controlling the sequential order and the amounts of neutral Cs atoms and Cs^+ ions deposited on graphene. We find, however, no such a gap-opening in graphene when Cs^+ ions of energy <100 eV are doped on SLG, where the π-band becomes gradually weaker and more diffused with increasing dose of Cs^+ ions.

2.3. Theoretical DFT Band Calculations Based on a Capacitor Model

Our DFT calculations for the changes in the π-band provide a plausible clue for the Cs^+-induced band gap opening. Fig. 2a shows the optimized atomic structure of the SLG grown on SiC(0001) surface used in our DFT calculations. We find the graphene-buffer interlayer distance *d*=3.4 Å, which agrees well with measured value.[30] The binding site for neutral Cs atoms on graphene is found to be the hollow site with binding energy E_b = 1.18 eV, which is much favored energetically over the top (1.09 eV) or bridge (1.04 eV) site. Because of the limitation of handling bare Cs^+ ions in the DFT calculations, we devise a simple capacitor model for the Cs^+-doped SLG system as schematically drawn in Fig. 2b, where the distance *d* and the interlayer electric field (E_{GB}) vary with the dose of Cs^+ ions. The doped Cs^+ ions on SLG form a positively charged layer with surface charge density ρ_{Cs}. As the Bader analysis suggests,[31] electrons are transferred from SiC substrate to the graphene and buffer layer to make the surface charge density of $-\rho_G$ and $-\rho_B$ respectively, while SiC is positively charged with $\rho_G + \rho_B$. The electric field E_{GB} between graphene and the buffer layer is then given by

$$E_{GB} = \frac{\rho_{Cs} - 2\rho_G}{2\varepsilon_0}, \quad (1)$$

where ε_0 is the vacuum permittivity. The whole system depicted in Fig. 2b is then equivalent to a parallel-plate capacitor with a surface charge density of $(\rho_{Cs} - 2\rho_G)/2$. The key idea in our capacitor model is that the change of the interlayer distance Δd represents the modified sublattice asymmetry by the dosed either Cs^+ ions or neutral Cs atoms[32] as confirmed in our calculation (not shown). One notices the asymmetry already existing even from the beginning when Δd=0, and increases with increasing Δd. The equilibrium distance *d* may be found when the energy loss ΔU from the reduced *d* (red curve in Fig. 2c) is balanced by the gain from the electrostatic energy,

$$\Delta U = \frac{1}{2}\varepsilon_0 E_{GB}^{\ 2} A\Delta d = \frac{(\rho_{Cs} - 2\rho_G)^2}{8\varepsilon_0} A\Delta d, \quad (2)$$

where *A* is the surface area of a supercell used in the DFT calculations. Our results presented in Fig. 2c show that *d* is indeed reduced by *Δd* =0.55 (green arrow) and 0.17 Å (blue arrow) upon the dose of one Cs^+ ion per 2×2 and 3×3 supercells, or equivalently 1.0 ML and 0.44 ML, respectively. Fig.s 2d-f reveal the calculated band structures of graphene on SiC(0001) surface for some values of *Δd*. The DP of SLG (*Δd*=0) is found at 0.45 eV. As seen in our measured π-bands in Fig. 1, we find that the π-band shifts down away from the Fermi level and opens a band gap, of which the size increases gradually with increasing *Δd* producing E_g=0.112 eV for *Δd*=0.5 Å. Though the absolute size of the band gap is quite different from the one observed, our calculation reveals a driving force of the band gap upon increasing *Δd*, the sublattice asymmetry in graphene.[32]

We also find that the charge density ρ_{Cs} (*>20* ρ_G) from the Cs^+ ions is significantly greater than ρ_G, the negative charge density of graphene transferred from SiC. This explains why no detectable band gap opens when neutral Cs atoms alone are adsorbed on SLG since *ΔU* becomes negligibly small for $-\rho_G$ of graphene as the only charge for E_{GB}. When neutral Cs atoms are added on the Cs^+ pre-added graphene, a new charge density ρ_G^* begins to form in graphene transferred from the SiC substrate in addition to ρ_G to achieve a new Bader's condition, $\nabla\rho$=0, along the surface normal because of the added Cs atoms.[31] Our core level data show the signature for the presence of ρ_G^* as discussed later. The gradual decrease of the band gap in Fig.s 1d-h appears since E_{GB} decreases gradually as the net charge density $\rho_{Cs}-2(\rho_G^*+\rho_G)$ in graphene decreases with increasing ρ_G^* as ϑ_{Cs} increases. The band gap eventually disappears when E_{GB} vanishes for a certain ϑ_{Cs} that makes $\rho_{Cs}-2(\rho_G^*+\rho_G)$=0. Experimentally this occurs when ϑ_{Cs}=1.0 ML as shown in Fig. 1h.

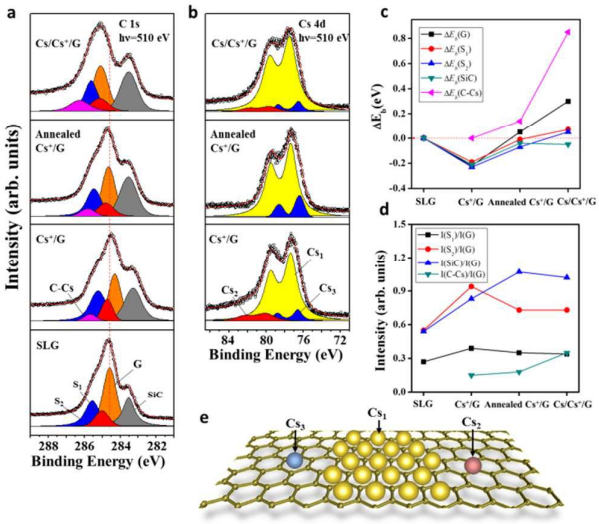

Fig. 3 Cs-induced changes in the core levels. (a), C 1s and (b), Cs 4d core-level spectra collected with synchrotron photons of energy 510 eV from the four different phases of graphene as in Figure 1. The annealing temperature T_a=300 °C, and the Cs coverage ϑ_{Cs}=1.2 ML for the $Cs/Cs^+/G$ phase. The red curves are the fit curves of the data points (empty circles), and the vertical dashed line indicates the G-subcomponent of SLG to guide eyes. The changes in binding energy ΔE_b and normalized spectral intensity (I) of C 1s are presented in (c) and (d), respectively. Three different components, Cs_1, Cs_2, and Cs_3, of Cs 4d in (b) are schematically drawn in (e) with Cs (large circles) bonded with carbons (small circles) at three distinct binding sites.

The characteristic changes in the C 1s and Cs 4d core levels presented in Fig. 3 for the four different phases of graphene; SLG, Cs^+/G, annealed Cs^+/G , and $Cs/Cs^+/G$ also suggest that the Cs^+-induced lattice asymmetry drives the band gap opening as discussed below. The C 1s from the SLG formed on SiC(0001) in Figure 3a has four subcomponents; G from carbons of graphene, S_1 and S_2 from carbons of the buffer layer bonded with and without Si atoms, and SiC from the substrate. The red solid curves are the fit-curves of the data points (empty circles). To estimate the relative abundance of graphene, we have used a conventional layer-attenuation model for core-level intensities.[33]

The dose of Cs^+ ions for the Cs^+/G phase immediately produces a new subcomponent, C-Cs (E_b=285.7 eV) in the C 1s, arising from Cs-bonded carbons at the expense of the reduced G component.[28] One also notices that the whole spectrum is uniformly shifted by about −0.20 eV toward the lower binding energy side as also seen in the valence band (Fig. 1b), arising from the reduced charge transfer from the substrate as mentioned earlier.[24] The Cs 4d core levels in Fig. 3b are best fitted with three subcomponents Cs_1, Cs_2, and Cs_3 suggesting three distinct bonding configurations as depicted in Fig. 3e. A spin-orbit splitting of 2.2 eV and a branching ratio of 0.77 between the Cs $4d_{3/2}$ and Cs $4d_{5/2}$ have been used to fit the Cs 4d spectra.[34] Since most alkali metals favour to occupy the hollow sites,[35,36] we ascribe the Cs_1 to the most abundant Cs atoms at the sites slightly off from the hollow sites, while the Cs_3 to the Cs atoms also at the off-hollow sites well isolated from its neighboring Cs

atoms.[37] The Cs atoms sitting at the off-symmetric hollow sites are favored to understand the five-times greater band gap (0.55 eV) observed than the calculated value of 0.11 eV (Fig. 2f) where no enhanced sublattice asymmetry due to the local bonding configuration is considered.

As seen in Fig. 1c, a band gap opens when the Cs^+/G is annealed at T_a=300 °C. Similar changes in the core levels appear also in Fig. 3. One first notices that all the subcomponents in the core levels shift toward the higher binding energy side, most remarkably by 0.27 eV for the G-subcomponent of the C 1s. We also observe a kind of 'healing effect' from the Cs 4d in Fig. 3b, where the weak Cs_2 disappears completely upon annealing while the Cs_1 and Cs_3 are increased correspondingly. The Cs_2 subcomponent represents the Cs atoms sitting at the unstable sites such as defects or the edges where more dangling bonds are available to make the Cs-C bonding stronger. Thus, the annealing brings the system into an equilibrium configuration with more Cs_1 and Cs_3 atoms, which naturally increases E_{GB} (or reduces *d*) to open a band gap. This explanation is consistent with the increased intensity of the SiC subcomponent of C 1s in Fig. 3a upon annealing because of the reduced *d*.[38]

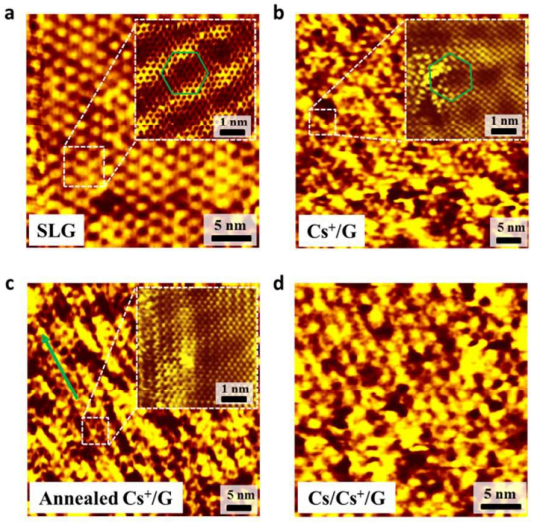

Fig. 4 Asymmetry in charge distribution. STM images from (a), SLG (30 nm×30 nm, V_t=−0.8 V, I_t=0.7 nA), (b), Cs^+/G (50 nm×50 nm, V_t=−0.1 V, I_t=0.4 nA), (c), annealed Cs^+/G (50 nm×50 nm, V_t=−0.1 V, I_t=0.3 nA), and (d), Cs/Cs^+/G (30 nm×30 nm, V_t=−0.045 V, I_t=0.4 nA). Inset in (a)–(c) show the magnified images of the region marked by the dashed boxes. One notices a preferred direction (green arrow) in (c) and (d), indicative of charge asymmetry, for the samples where a band gap is observed.

In fact, the ratio I(SiC)/I(G) in Fig. 3c is found to continue to increase with further annealing. The equilibrium configuration with no Cs_2 atoms for the annealed Cs^+/G system, therefore, has a minimum value for *d,* or a maximum asymmetry for the A and B sublattices of graphene, and thus reveals a maximum band gap $E_g \geq 0.55$ eV (Fig. 1c).

As described, the band gap decreases gradually upon adding neutral Cs atoms to form the Cs/Cs^+/G system (Fig.s 1d-g), and disappears completely at ϑ_{Cs}=1.0 ML (Fig. 1h). The corresponding changes in the core levels shown in Fig. 3a reveal a prominent shift of the subcomponent C-Cs by ΔE_b=+0.71 eV while that of G by ΔE_b=+0.25 eV, much greater than the shifts (≤0.07 eV) of other subcomponents. Such remarkable shifts toward the higher energy side strongly indicate a significant change in charge distribution near the carbon atoms induced not only by neutral Cs atoms but also by the extra charge ρ_G^* from the SiC substrate. The addition of neutral Cs atoms on the Cs^+/G sample, therefore, reduces E_{GB}, and also the charge asymmetry. This explains why the band gap decreases with increasing ϑ_{Cs}, and disappears completely at ϑ_{Cs}=1.0 ML when E_{GB}=0. The G-subcomponent of C 1s also restores its value of the SLG with increasing ϑ_{Cs} as observed (Fig. 3b). We further notice that any excess Cs atoms beyond ϑ_{Cs}=1.0 ML causes to shift the DP further away from the Fermi energy revealing an n-doping effect as seen in Fig. 1i.

Now we find evidence for the Cs-induced sublattice asymmetry in our STM images presented in Fig. 4 obtained from the four different phases of graphene SLG, Cs^+/G, annealed Cs^+/G , and Cs/Cs^+/G. The well-known 6×6 pattern (green hexagon) is seen from the SLG (Fig. 4a) reflecting the underlying 6√3×6√3 reconstruction of the buffer layer with unsaturated C atoms.[39] The Cs^+ ions are found to sit rather randomly at the rim regions of the Moiré pattern appearing as disordered bright protrusions in Fig. 4b. Interestingly no superstructure of either 1×1 or √3×√3 reported for the neutral Cs-adsorbed graphene is seen, indicating the distinct C-Cs bonding configurations from the one reported earlier.[29,40] One, however, notices some interference pattern near Cs^+ ions as for the Ar^+ ions on graphene,[24,41] suggesting the formation of some defects by Cs^+ ions such as the Cs_2 atoms to cause the uniform shift in the π-band (Fig. 1b) and in the core levels (Fig. 3a). From the STM images in Fig. 4c for the annealed Cs^+/G sample, one notices some stripes along a

preferred direction (green arrow), an indicative of a certain charge asymmetry from the Cs atoms sitting at the off-symmetric hollow sites, which may cause the opening of a band gap. Interestingly this asymmetry in the STM images begins to disappear locally as neutral Cs atoms are added on the Cs^+/G as seen in Fig. 4d, which is consistent with the reducing band gap in the π-band. This confirms that the Cs^+-induced charge asymmetry among carbon atoms drives the opening of a band gap and the corresponding changes in the core levels.

3. Conclusions

In summary, by using slow Cs^+ ions, we demonstrate the gap engineering for the SLG formed on SiC(0001) surface. Our ARPES data for the linear π-band of graphene reveals the opening of a band gap of which the size can be artificially fine-tuned up to E_g=0.68 eV by adjusting the amount of the doped Cs^+ ions. We also show that the Cs^+-induced band gap can also be closed gradually by adding neutral Cs atoms, and be opened again by additional Cs^+ ions in a proper sequential order, thus illustrating a reproducible on/off switching capability of the band gap of graphene. Our core level data (C 1s and Cs 4d) combined with STM images consistently support that the charge asymmetry among carbon atoms induced by Cs^+ ions drives the band gap opening in graphene. Our DFT calculations adopting a capacitor model to simulate the Cs^+-doped graphene indeed reveal that the reduced interlayer distance *d* between graphene and the buffer layer, which is equivalent to the increased sublattice asymmetry, opens a band gap at the K-point up to E_g=0.112 eV for Δd=0.5 Å. This simple capacitor model, therefore, explains most of the prominent changes in the π-band as well as in the core levels induced by the doped Cs^+ ions and neutral Cs atoms including the opening and fine-tuning the size of a band gap in graphene. We thus present a reliable and practical means of engineering the band gap of graphene, which should play a pivotal role in advancing the graphene-based nano-electronic technology.

Acknowledgements

This work was supported by the National Research Foundation of Korea (NRF) grant funded by the Korea Government (NRF-2015R1A5A1009962), by the Ministry of Science, ICT and Future Planning (NRF-2013R1A1A2005598), and also by the Ministry of Education (2014R1A1A2054592). Jhi acknowledges support by the SRC Center for Topological Matter (2011-0030789) and the LG Yonam Culture Foundation.

References

1 K. S. Novoselov, A. K. Geim, S. V. Morozov, D. Jiang, Y. Zhang, S. V. Dubonos, I. V. Grigorieva, A. A. Firsov, *Science* 2004, ***306***, 666.
2 K. S. Novoselov, A. K. Geim, S. V. Morozov, D. Jiang, M. I. Katsnelson, I. V. Grigorieva, S. V. Dubonos, A. A. Firsov, A. A. *Nature* 2005, ***438***, 197.
3 Y. Zhang, Y. W. Tan, H. L. Stormer, P. Kim, *Nature* 2005, ***438***, 201.
4 A. K. Geim, K. S. Novoselov, *Nat. Mater*. 2007, ***6***, 183.
5 E. J. Duplock, M. Scheffler, P. J. D. Lindan, *Phys. Rev. Lett.* 2004, ***92***, 225502.
6 Y. W. Son, M. L. Cohen, S. G. Louie, *Phys. Rev. Lett.* 2006, ***97***, 216803.
7 X. Liang, Z. Fu, S. Y. Chou, *Nano Lett.* 2007, ***7***, 3840.
8 Y.-M. Lin, C. Dimitrakopoulos, K. A. Jenkins, D. B. Farmer, H.-Y. Chiu, A. Grill, Ph. Avouris, *Science* 2010, ***327***, 662.
9 F. Xia, D. B. Farmer, Y.-M. Lin, Ph. Avouris, *Nano Lett.* 2010, ***10***, 715.
10 C. Berger, Z. Song, X. Li, X. Wu, N. Brown, C. Naud, D. Mayou, T. Li, J. Hass, A. N. Marchenkov, E. H. Conrad, P. N. First, W. A. de Heer, *Science* 2006, ***312***, 1191.
11 M. Y. Han, B. Özyilmaz, Y. Zhang, P. Kim, *Phys. Rev. Lett.* 2007, ***98***, 206805.
12 T. Ohta, A. Bostwick, T. Seyller, K. Horn, E. Rotenberg, *Science* 2006, ***313***, 951.
13 Y. Zhang, T. Tang, C. Girit, Z. Hao, M. Martin, A. Zettle, M. F. Crommie, Y. Shen, F. Wang, *Nature* 2009, ***459***, 820.
14 S. Niyogi, E. Bekyarova, M. E. Itkis, H. Zhang, K. Shepperd, J. Hicks, M. Sprinkle, C. Berger, C. N. Lau, W. A. de Heer, E. H. Conrad, R. C. Haddon, *Nano Lett.* 2010, ***10***, 4061–4066.
15 A. *J.* Grüneis, *Phys.*: *Condens. Matter* 2013, ***25***, 043001.
16 R. Balog, B. Jørgensen, L. Nilsson, M. Andersen, E. Rienks, M. Bianchi, M. Fanetti, E. Lægsgaard, A. Baraldi, S. Lizzit, Z. Sljivancanin, F. Besenbacher, B. Hammer, Th. Pedersen, P. Hofmann, L. Hornekær, *Nat. Mater.* 2010, ***9***, 315.
17 J. Berashevich, T. Chakraborty, *Phys. Rev. B* 2009, ***80***, 033404.
18 C. Coletti, C. Riedl, D. S. Lee, B. Krauss, L. Patthey, K. von Klitzing, J. H. Smet, U. Starke, *Phys. Rev. B* 2010, ***81***, 235401.
19 D. C. Elias, R. R. Nair, T. M. G. Mohiuddin, S. V. Morozov, P. Blake, M. P. Halsall, A. C. Ferrari, D. W. Boukhvalov, M. I. Katsnelson, A. K. Geim, K. S. Novoselov, *Science* 2009, ***323***, 610.
20 M. Jaiswal, C. H. Y. X. Lim, Q. Bao, C. T. Toh, K. P. Loh, B. Özyilmaz, *ACS Nano* 2011, ***5***, 888.
21 S. J. Sung, P. R. Lee, J. G. Kim, M. T. Ryu, H. M. Park, J. W. Chung, *Appl. Phys. Lett.* 2014, ***105***, 081605.
22 N. Li, G. Lee, J. W. Yang, H. Kim, M. S. Yeom, R. H. Scheicher, J.-S. Kim, K.-S. Kim, *J. Phys. Chem. C* 2013, ***117***, 4309.
23 S. Y. Zhou, G.-H. Gweon, A. V. Fedorov, P. N. First, W. A. de Heer, D.-H. Lee, F. Guinea, A. H. Castro Neto, A Lanzara, *Nat. Mater.* 2007, ***6***, 770.
24 H. Jee, K. H. Jin, J. H. Han, H. N. Hwang, S. H. Jhi, Y. D. Kim, C. C. Hwang, *Phys. Rev. B* 2011, ***84***, 075457.
25 M. Papagno, S. Rusponi, P. M. Sheverdyaeva, S. Vlaic, M. Etzkorn, D. Pacilé, P. Moras, C. Carbone, H. Brune, *ACS Nano* 2012, ***6***, 199.
26 C. Jeon, H. Shin, I. Song, M. Kim, J. Park, J. Nam, D. Oh, S. Woo, C. C. Hwang, C.-Y. Park, J. R. Ahn, *Sci. Rep.* 2013, ***3***, 2725.

27 A. Bostwick, F. Speck, Th. Seyller, K. Horn, M. Polini, R. Asgari, A. H. MacDonald, E. Rotenberg, *Science* 2010, ***328***, 999.
28 S. Watcharinyanon, C. Virojanadara, L. I. Johansson, *Surf. Sci.* 2011, ***605***, 1918.
29 M. Petrović, I. Šrut Rakić, S. Runte, C. Busse, J. T. Sadowski, P. Lazić, I. Pletikosić, Z.-H. Pan, M. Milun, P. Pervan, N. Atodiresei, R. Brako, D. Šokčević, T. Valla, T. Michely, M. Kralj, *Nat. Commun.* 2013, ***4***, 2772.
30 F. Varchon, R.Feng, J. Hass, X. Li, B. Ngoc Nguyen, C. Naud, P. Mallet, J.-Y. Veuillen, C. Berger, E. H. Conrad, L. Magaud, *Phys. Rev. Lett.* 2007, ***99***, 126805.
31 G. Henkelman, A. Arnaldsson, H. Jónsson, *Comput. Mater. Sci.* 2006, ***36***, 354.
32 S. Kim, J. Ihm, H. J. Choi, Y. W. Son, *Phys. Rev. Lett.* 2008, ***100***, 176802.
33 K. V. Emtsev, F. Speck, Th. Seyller, L. Ley, J. D. Riley, *Phys. Rev. B* 2008, ***77***, 155303.
34 D. S. Lin, T. Miller, T.-C. Chiang, *Phys. Rev. B* 1991, ***44***, 10719.
35 K. T. Chan, , J. B. Neaton, M. L. Cohen, *Phys. Rev. B* 2008, ***77***, 235430.
36 G. Profeta, M. Calandra, F. Mauri, *Nature. Phys.* 2012, ***8***, 131.
37 K. H. Jin, S. M. Choi, S. H. Jhi, *Phys. Rev. B* 2010, ***82***, 033414.
38 J. Chen, T. Shi, T. Cai, T. Xu, L. Sun, X. Wu, D. Yu, *Appl. Phys. Lett*. 2013, ***102***, 103107.
39 J.-Y. Veuillen, F. Hiebel, L. Magaud, P. Mallet, F. *J.* Varchon, *Phys. D*: *Appl. Phys.* 2010, ***43***, 374008.
40 C.-L. Song, B. Sun, Y. Wang, Y. Jiang, L. Wang, K. He, X. Chen, P. Zhang, X. C. Ma, Q. K. Xue, *Phys. Rev. Lett.* 2012, ***108***, 156803.
41 G. M. Rutter, J. N. Crain, N. P. Guisinger, T. Li, P. N. First, J. A. Stroscio, *Science* 2007, ***317***, 219.
42 S. Y. Shin, C. G. Hwang, S. J. Sung, N. Kim, H. S. Kim, J. W. Chung, *Phys. Rev. B* 2011, ***83***, 161403.
43 S. J. Sung, J. W. Yang, P. R. Lee, J. G. Kim, M. T. Ryu, H. M. Park, G. Lee, C. C. Hwang, K.-S. Kim, J.-S. Kim, J. W. Chung, *Nanoscale* 2014, ***6***, 3824.
44 G. Kresse, J. Furthmüller, *Phys. Rev. B* 1996, ***54***, 11169.
45 G. Kresse, D. Joubert, *Phys. Rev. B* 1999, ***59***, 11.
46 J. P. Perdew, K. Burke, M. Ernzerhof, *Phys. Rev. Lett.* 1996, ***77***, 3865.
47 A. Tkatchenko, M. Scheffler, *Phys. Rev. Lett.* 2009, ***102***, 073005.